

Photovoltaic Panel Defect Detection Algorithm based on Improved YOLOv8s

Ziqing Song^{1,*}, Yupeng Yao², Jingbin Yang³

¹ College of Zhan Tianyou, Dalian Jiaotong University, Dalian 116000, Liaoning, China

² College of Zhan Tianyou, Dalian Jiaotong University, Dalian 116000, Liaoning, China

³ Institute of Robotics and Intelligent Equipment, School of Mechanical Engineering, Tianjin University of Technology and Education, Tianjin 300222, China

*Corresponding Author: Ziqing Song

Abstract

Aiming at the problems of insufficient accuracy and large parameter amount of the existing YOLO model in defect detection, an improved YOLOv8s algorithm was proposed for photovoltaic panel defect detection. On the basis of retaining the backbone network structure, the full-dimensional dynamic convolutional ODConv is introduced, ODConv is combined with C2f, and the C2f_ODConv module is constructed to replace C2f of the neck small target layer, which effectively improves the feature extraction ability of small targets. At the same time, the TripletAttention mechanism is embedded to enhance the model's attention to subtle defects. Finally, we introduce the Focaler-IoU loss function. It integrates Focal Loss and dynamically weights difficult samples to improve bounding box regression accuracy. The results show that the mAP of the improved model is increased from 90.6% to 94.2%, and the calculation amount is reduced to 8.8GFLOPs, especially in the "cover" defect detection, the mAP is increased by 9.1%. Compared with other mainstream algorithms, the proposed method has advantages in accuracy and speed, and is suitable for automatic inspection and defect identification tasks of photovoltaic power stations.

Keywords

Photovoltaic Panel Defect Detection; Yolov8; Dynamic Convolution; Attention Mechanism.

1. Introduction

Under the background of promoting the implementation of the "double carbon" goal, the photovoltaic power generation industry has developed rapidly, accounting for 24.83% of the total energy in the country, and photovoltaic power stations have become one of the main sources of renewable energy. Solar photovoltaic panel is the core component of photovoltaic power station^[1], Due to outdoor exposure, these panels inevitably accumulate debris and develop defects. If these problems can not be found in time and make the corresponding treatment, it will inevitably affect the photovoltaic power station. According to statistics, even a small amount of foreign body attachment can also have a greater impact on the power generation rate and life of photovoltaic panels, for large-scale photovoltaic power stations, this will undoubtedly produce greater economic losses. Common PV panel failures - including physical damage, electrical shorts, and grid fractures - first disrupt normal operation. This leads to significant losses in power generation efficiency and overall plant stability. The consequences extend to reduced system reliability, shortened equipment lifetime, heightened

safety risks, and increased operational costs.(e.g., reducing the need for aerial work). Therefore, it is of great significance to accurately and efficiently detect the status of photovoltaic panels^[2]. Traditional detection mainly relies on manual inspection, which has the uncertainty of subjective judgment. After a period of time, it will lead to low efficiency due to fatigue, high cost, and difficult to meet large-scale demand. Many scholars have devoted their efforts to this research. Li Bing et al^[3]. proposed a multi-scale photovoltaic panel defect detection method based on attention fusion to solve the problems of large size variation and low detection accuracy of photovoltaic panel defects in complex infrared background. Yingchun Guan et al^[4].^[4] proposed to extract defect features through UAV imaging and segment defect images using gray level co-occurrence matrix to achieve high-precision detection of photovoltaic plant panel defects in view of the problem of unclear results in panel defect detection of photovoltaic plant. Liao Kun et al^[5].proposed a photovoltaic panel identification and extraction model and a quantitative analysis model of ash accumulation state based on field images to realize the intelligent perception of photovoltaic panel ash accumulation state, and the accuracy of the recognition model reached 81%. Liu Xiaoxiong et al^[6].^[6] used an algorithm called AKAZE to stitch multiple images into a panorama, and then segmented the photovoltaic panel from the picture by image processing technology. Then the deep learning model is used to identify different types of defects on the PV panel. The experimental results show that the accuracy of defect detection is improved without touching the photovoltaic panel.

Recent advances in deep learning and image processing have enabled more effective defect detection in solar panels. Compared with traditional methods, deep learning methods have higher accuracy and stronger robustness after learning a large number of samples^[7]. At present, deep learning and object detection methods are mainly divided into the following two categories: one is a one-stage algorithm, such as YOLO^[8], which directly predicts the object box and category, and the other is a two-stage object detection algorithm, such as Faster-RCNN^[9], which first generates candidate regions and then performs classification and regression. However, whether it is a one-stage algorithm or a two-stage algorithm, many scholars use different deep learning models to apply to the defect detection of photovoltaic panels, which improves the overall detection accuracy and work efficiency.For example, Yang Changchun et al^[10]. achieve a balance between high efficiency and high performance through StarNet network architecture, SPPF-AM module, triple attention mechanism, C2f_DSConv2D and other technologies to solve the problems of low accuracy, high computation and large parameter amount in distributed photovoltaic panel defect detection. Aiming at the surface defect detection problem of solar cells in the manufacturing and transportation process, Zihan Zhang et al^[11]. proposed a deep learning model combining the C2f module of YOLOv8 and the lightweight attention module of Hybrid Local Channel Attention (MLCA) to improve the reliability and accuracy of defect detection. The above methods have achieved certain results in the accuracy of photovoltaic panel defect detection, but there is still a large room for improvement in the lightweight detection model.

YOLOv8 has the advantage of modularity, which can be optimized and customized on this basis. This paper proposes an enhanced YOLOv8s model for solar panel defect detection. By optimizing the network architecture, we boost detection accuracy and inference speed while preserving the model's lightweight design. In order to enable the model to better detect non-obvious defects. The main contributions of this paper are:

- 1) The C2f_ODConv module is designed in the feature fusion network to replace the C2f module in the small target layer of the neck network to improve the accuracy of the model.
- 2) The second enhancement applies TripletAttention to small-target processing. This mechanism improves discriminative feature learning for tiny objects.

3) The Focaler loss function is integrated into the original loss function IoU to enhance the fitting ability of the bounding box loss, and realize the lightweight transformation of the model and the improvement of recognition accuracy.

2. YOLOv8 Model and its Improvement

2.1. YOLOv8 Model

YOLOv8 is a real-time object detector released by Ultralytics in January 2023. It uses a single-stage deep learning architecture, and its structure is shown in Figure 1. According to the depth of the network and the width of the feature map, it can be divided into five versions such as YOLOv8-n, s, and m^[12].

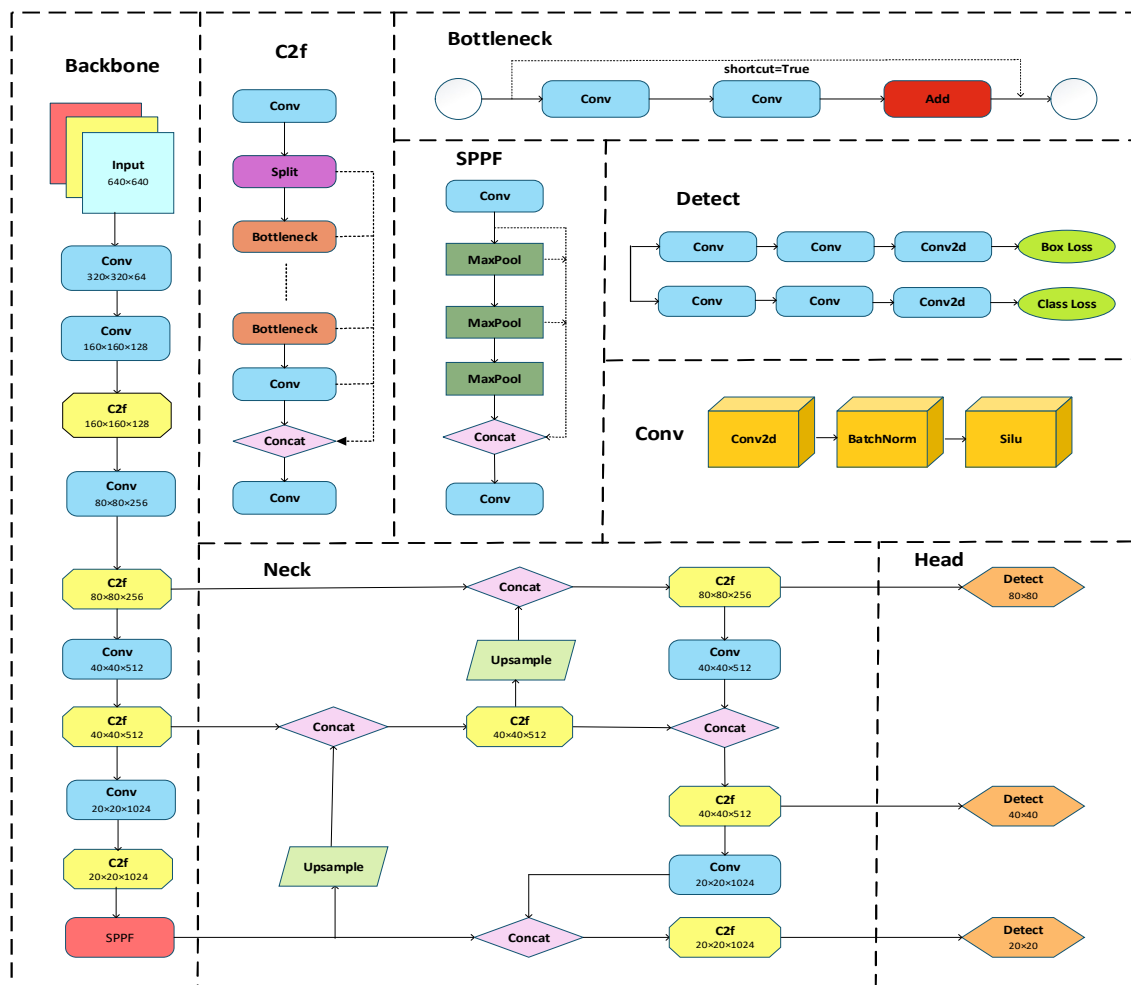


Figure 1. Structure of YOLOv8 network

The backbone network consists of Conv, C2f and SPPF modules. The C2f module is used to replace the traditional C3 module, which combines the efficiency of YOLOv5-C3 and the gradient flow optimization mechanism of YOLOv7-ELAN, which is lightweight and can significantly enhance the feature representation ability. At the same time, the module retains the SPPF layer (fast spatial pyramid pooling) to expand the model receptive field. The model can better extract spatial features and accelerate multi-scale context information aggregation. Neck is composed of Upsample, Concat and C2f. Multi-scale fusion is realized by integrating multi-scale information for feature reorganization to prepare for subsequent detection. Head uses decoupling head design to predict the target center point and width and height, which is

used for separation classification and positioning tasks. The dynamic Anchor in YOLOv5/v7 is abandoned, and the more advanced Anchor-free^[13] is combined. This mechanism can directly return the target position and directly predict the target center point and scale, so as to avoid redundant calculation. In this paper, Yolov8 model is improved to improve the effect of photovoltaic panel defect detection. At the same time, on the premise of ensuring the original amount of calculation and parameter lightweight, the model improves the detection accuracy.

2.2. YOLOv8 Model Improvemen

In this paper, Yolov8 model is improved in the following aspects, and the improved model is shown in Figure 2.

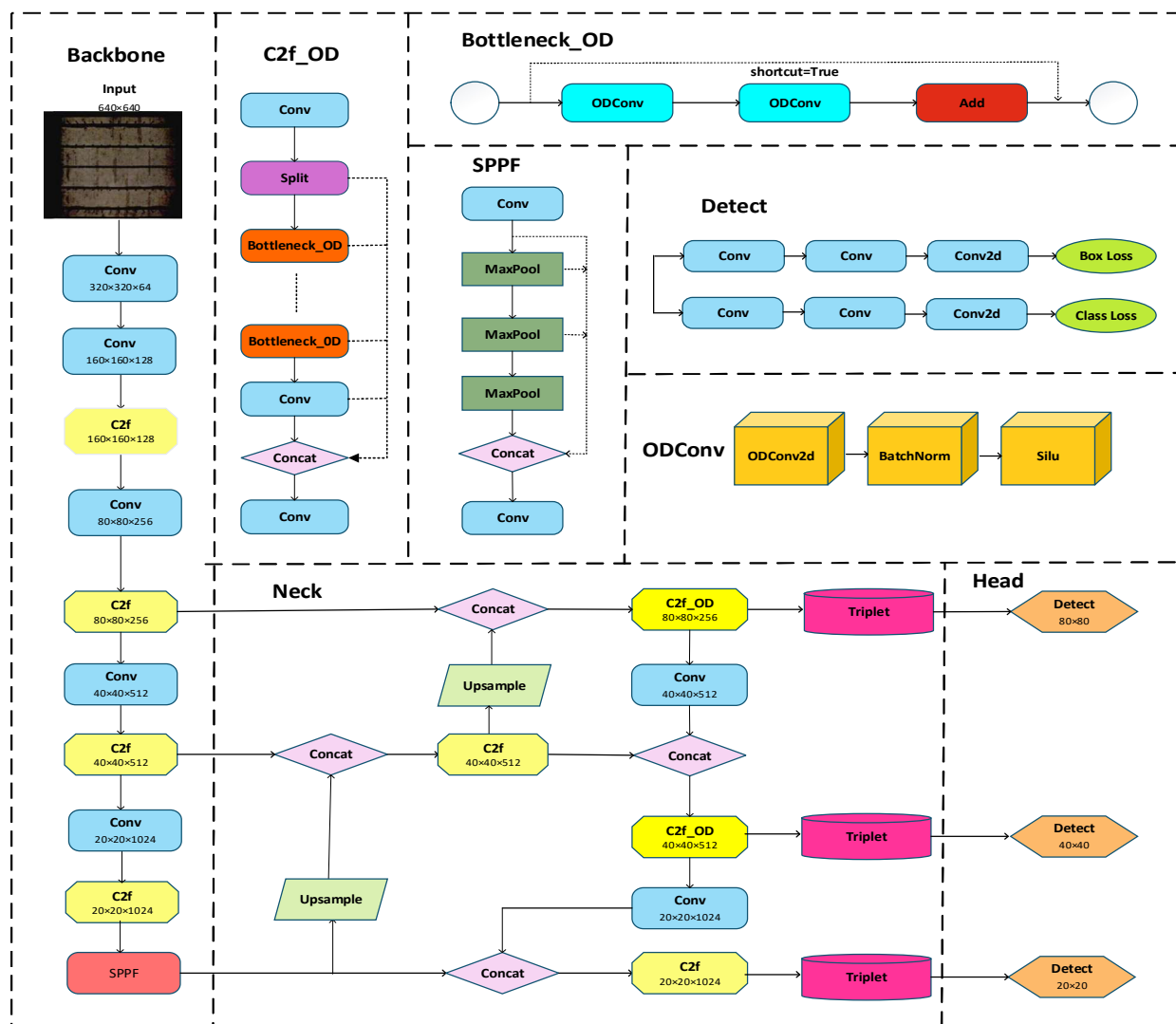


Figure 2. Structure of improved YOLOv8 network

2.2.1. Improvements To The C2f Module

As the backbone module of the network structure, the C2f module of Yolov8 is usually located in the deep layer, but the deep feature map has a large receptive field, which is more suitable for large and medium targets. For small targets of photovoltaic panel defects, it is difficult to be effectively captured, so its insensitivity leads to low detection accuracy of small targets. The ODConv convolution is introduced to combine with the C2f module to form the C2f_ODConv module to replace C2f in the original neck network. ODConv is named Omni-Dimensional Dynamic Convolution, and it adopts four-dimensional dynamic attention (that is, space size, number of input channels, number of output channels and convolution kernel). Its structure is

shown in Figure 3. The four dimensions complement and cooperate to maximize the flexibility of convolution kernel [14]. It is because this mechanism reduces its computation and improves its efficiency. And as a plug and play module, it is easy to combine with any module in the network, which can significantly improve the network performance.

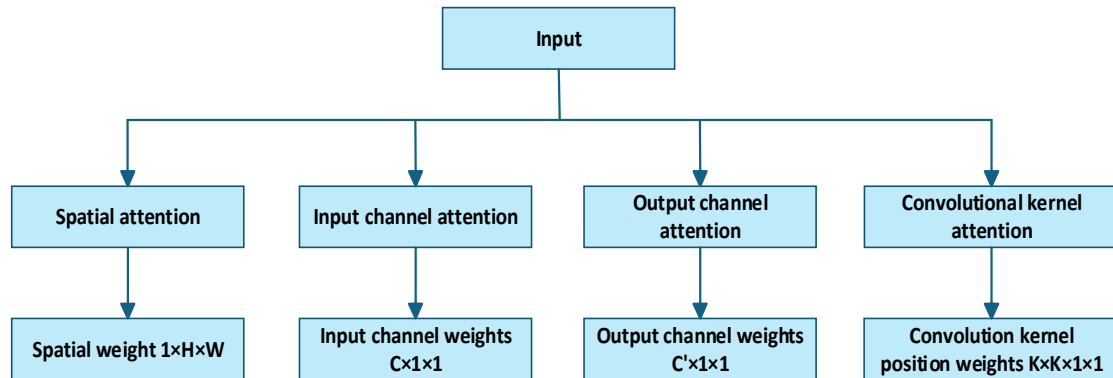


Figure 3. 4D Dynamic Attention in ODConv

In the proposed model, the convolution in the Bottleneck structure of the C2f module is replaced by ODConv to obtain the C2f_ODConv module, and the specific structure is shown in Figure 4.

The backbone network part C2f was retained, and C2f_OD was used to replace the C2f module of the small target layer in the neck network part to help the model perform feature enhancement at a smaller level and improve the accuracy value of the model.

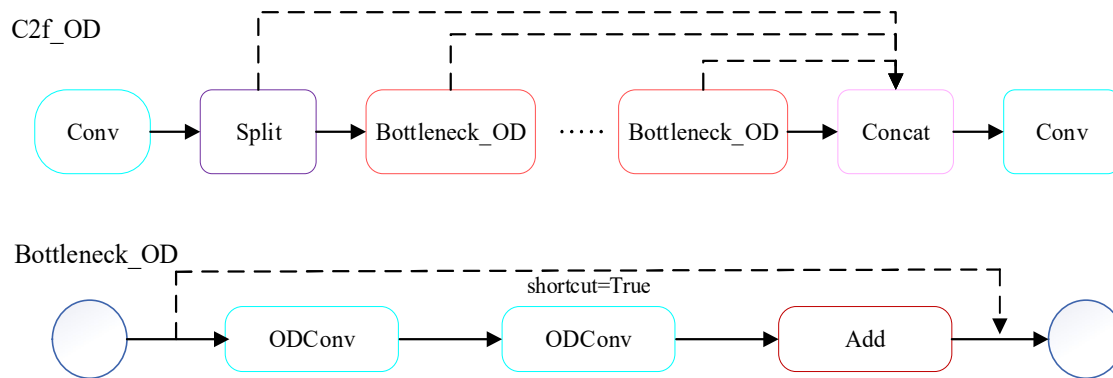


Figure 4. C2f_OD, Bottleneck_OD structure diagram

2.2.2. Improving The Attention Mechanism.

In order to further improve the performance of YOLOv8s object detection algorithm, this paper introduces TripletAttention module, which is a lightweight attention mechanism originally proposed in 2018. The TripletAttention module is inspired by the idea that three people observe a picture from different angles at the same time. The core idea is to automatically assign an appropriate weight to each channel by learning the relationship between channels, so that the model can better focus on and utilize important feature information and improve the representation ability and robustness of the model[15]. The TripletAttention branch structure is shown in Figure 5.

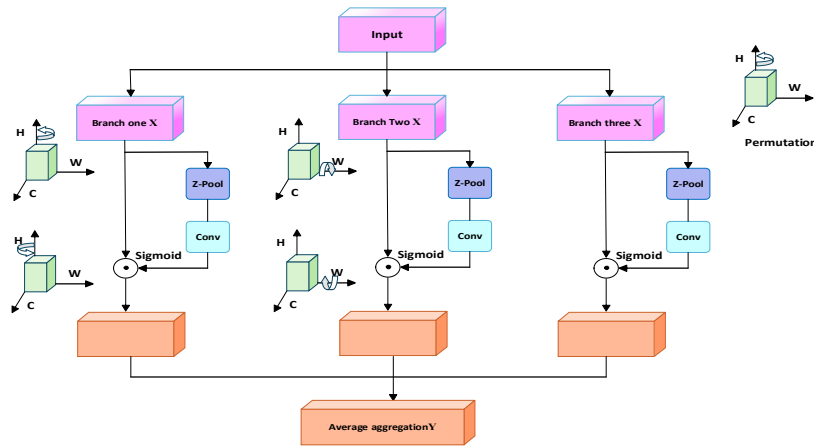


Figure 5. Triplet structure diagram

In the original official model of Yolov8, the common attention mechanism module is not introduced. Therefore, in the model of this paper, a TripletAttention attention mechanism is embedded after the modified C2f module in the small target layer and the middle target layer of the neck part, and the large target layer remains unchanged. The structure is shown in Figure 6.

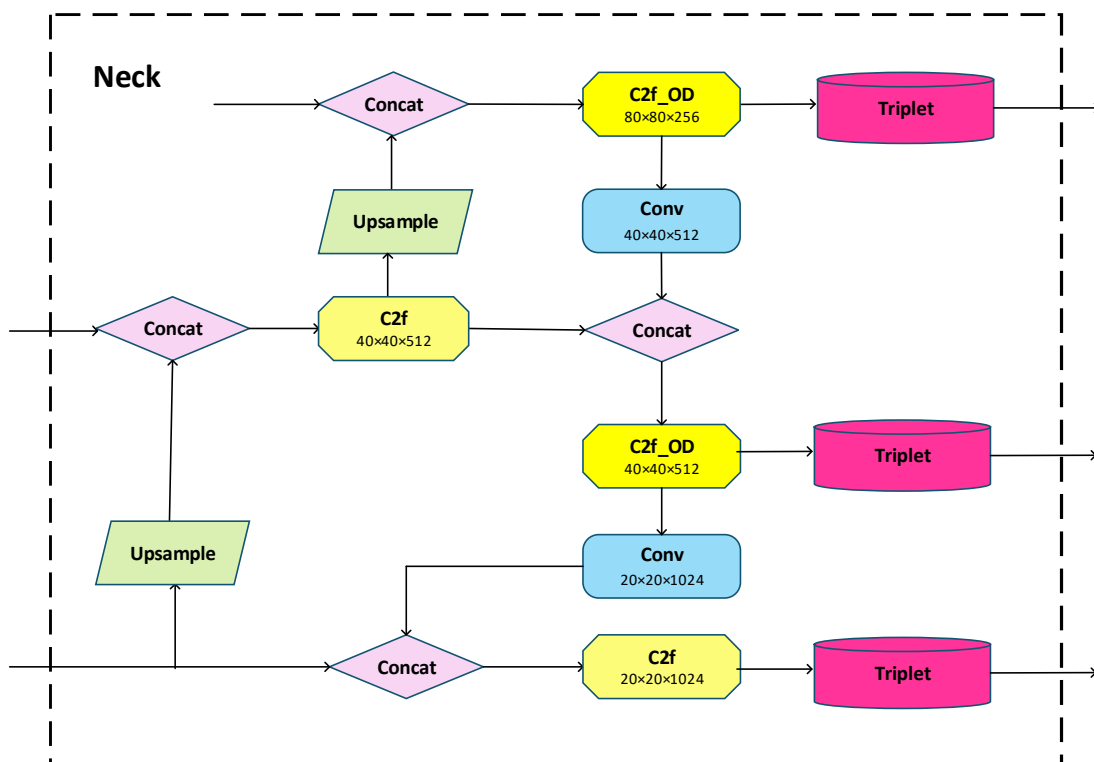


Figure 6. Structure diagram after adding Triplet

The above improvements can help the model to perform additional feature enhancement when predicting small objects, and then significantly improve the accuracy of small objects.

2.2.3. Improvements to the Loss Function.

The original Yolov8 model uses the following Loss functions for object detection: Class Loss, Box Loss, and Objectness Loss^[16]. However, for the detection of photovoltaic panels, especially the detection of small target defects, there are still certain limitations, such as: ① the detection sensitivity of small targets is not high, photovoltaic small target defects generally only account

for a few pixels, and their receptive fields are 8×8 , 16×16 , and 32×32 respectively in the multiple down-sampling process. However, the anchor-free mechanism of YOLOv8 cannot adequately capture tiny features, so the small target features of PV panel defects are severely diluted. (2) Because the surface texture of the photovoltaic panel is complex, the pictures taken will appear grid lines, reflections, etc., which are easy to be misdetected. The classification loss is insufficient to detect similar texture defects, so the regression gradient of the loss function is submerged, affecting the accuracy of small targets.

To solve the above two problems, the Focaler-IoU loss function is added in this paper. Focaler-IoU was proposed in 2024, The formula is as follows: Equation (1), and its core improvement is to transfer the idea of Focal Loss to the bounding box regression task, and dynamically adjust the regression loss weights of difficult samples to solve the sample imbalance problem. The basic principles of Focaler-IoU are as follows: ① Focus on different regression samples, because the loss of IoU is reconstructed by linear interval mapping, which realizes the attention of different samples and can achieve high detection ability. ② Focaler-IoU addresses how easy or hard sample distribution affects bounding box regression. It adapts Focal Loss's dynamic weighting to prioritize samples by difficulty. ③ Focaler-IoU makes up for the shortcomings of the existing bounding box regression methods through its unique method.

$$\text{IoU}^{\text{focaler}} = \begin{cases} 0, & \text{IoU} < d \\ \frac{\text{IoU}}{u-d}, & d \leq \text{IoU} \leq u \\ 1, & \text{IoU} > u \end{cases}, \quad (1)$$

It adjusts the loss according to the value of IoU: when IoU is less than a lower threshold d , it is considered as a difficult sample and the weight is reduced, and the loss is 0. When the IoU is greater than an upper threshold u , it is regarded as a simple sample and the weight is enhanced, and the loss is 1. When the IoU is between d and u , the scale is linear and the final loss function is defined as Equation (2),

$$\mathcal{L}_{\text{Focaler-IoU}} = 1 - \text{IoU}^{\text{focaler}} \quad (2)$$

3. Experimental Analysis and Results

3.1. Dataset

The data set used in this experiment is the photovoltaic panel foreign body and defect pictures obtained by inversion and rotation expansion, removal and integration based on the network public data set, and labeling software is used to label the defects. The image has a resolution of 640×640 pixels and is saved in "JPG" format. A total of 3402 images are included, which are divided into five categories: scratch, broken, covered, black heart and short circuit. Examples of various categories are shown in Figure 7 as follows:

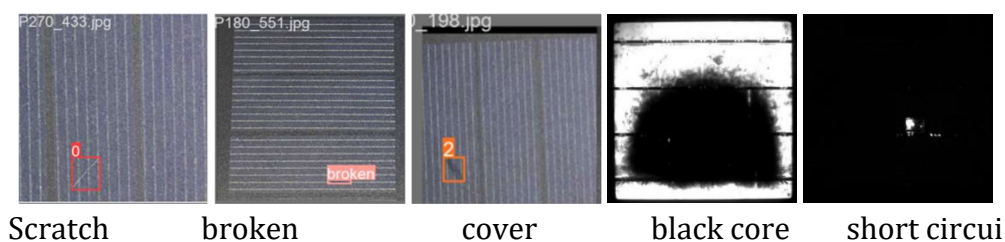


Figure 7. Examples of each defect category

3.2. Experimental Environment and Parameter Configuration

The experiment uses windows10 operating system, NVIDIA RTX A16 graphics card, and python1.8, CUDA11.3 and Pytorch1.10 deep learning frameworks. No pre-trained weights were used and automatic mixed-precision training was disabled, the Batch size of the dataset was set to 16 and the Epochs setting was changed to 150 during training. SGD is chosen as the optimizer, and the learning rate decays linearly to 0 as the iterations go on. Default values are used for the other parameters. The dataset of the experiment was randomly divided into a training set and a validation set according to the ratio of 8:2, that is, 2722 images in the training set and 680 images in the validation set. Other specific parameters are shown in Table 1 below.

Table 1. Experimental parameter table

Parameter names	Parameter values
lr	0.01
Momentum	0.937
Weight Decay	0.005
Size	640*640

3.3. Evaluation Index

In this paper, Precision, average precision, mean average precision, Param (number of parameters), and GFLOPs are used as the evaluation indicators of object detection performance, as follows:

Precision: This is the fraction of examples that are actually correct, out of all the examples that the model predicted and defined as correct. When the Precision is higher, it means that there are fewer false detections. The formula is given in Equation (3). TP (True Positive) means that the model can correctly detect the target box and define it as a photovoltaic panel defect, and the target area is indeed defined as a defect, that is, the true correct samples are defined as the correct number of samples. FP (False Positive) means that the model wrongly detects the target box and defines it as a photovoltaic panel defect, when the target area does not have the defined defect, that is, the number of wrong samples is defined as the correct samples.

$$P = \frac{TP}{TP+FP} \quad (3)$$

Average precision: This is the integral area of a pointer to a class at different recall rates. As shown in Equation 4.

Mean average precision: It is computed by averaging the individual average precision (AP) scores across all n classes. Specifically, it sums the AP values for each category and divides by n, providing a comprehensive evaluation metric for multi-class object detection systems. The higher the mAP value, the better the comprehensive performance of the model for each category detection. s shown in Equation 5.

$$AP = \int_0^1 P(R) dR \quad (4)$$

$$mAP = \frac{\sum_{i=0}^n AP(i)}{n} \quad (5)$$

3.4. Experimental Results and Analysis

3.4.1. Improvement and Comparison Experiments of C2f Module

In order to verify that the modified C2f_OD module can achieve the best model effect in which position, this subsection carries out comparative tests on the original Yolov8 model, replacing all C2f models of the backbone network, replacing all C2f models of the neck, and replacing only the C2f model of the small target layer of the neck. The experimental results are shown in the following Table 2. After replacing all ODConv in the backbone network, the number of parameters is greatly increased, and the overall mAP is improved. After replacing all Cf in the backbone, the number of parameters increases and the overall mAP improves slightly. After replacing all C2f in the neck, the number of parameters increased slightly, and the overall mAP improved. After replacing only the small target layer C2f in the neck, the number of parameters remains almost the same, and the overall mAP is improved. Therefore, the improved C2f_OD module is only used for replacement in the small object detection layer as an optimization scheme for the model.

Table 2. C2f module improvement comparison test table

Module	Param/($\times 10^6$)	GFLOPs	mAP/%
Yolov8	11.137535	28.8	90.6
v8s(all ODConv)	22.219750	27.4	92.5
v8s(all C2f_OD)	14.552139	25.5	91.3
v8s(neck C2f_OD)	13.930995	8.4	93.1
v8s(Small neck C2f_OD)	11.302777	8.6	92.3

3.4.2. Improvement and Comparative Experiment of Attention Mechanism Module

Table 3. Attention improvement comparison test

Module	Param/($\times 10^6$)	GFLOPs	mAP/%
Yolov8	11.137535	28.8	90.6
FocalModulation	11.550210	29.1	93.5
iRMB	11.300671	11.9	93.2
HAttention	21.980975	9.3	93.1
TripletAttention	11.138435	9.0	93.7

In order to verify the influence of different attention mechanisms on the performance of the model, FocalModulation, HAttention, iRMB and TripletAttention are introduced on the basis of the original improved model for comparison experiments, and the experimental results are shown in Table 3. The experimental results show that all attention mechanisms significantly improve the mAP of the model. Among them, TripletAttention is 93.7%, which is 3.1% higher than the original model's 90.6%. FocalModulation and iRMB were the second, reaching 93.5% and 93.2% respectively. HAttention is 93.1%. In terms of parameters, the parameters of FocalModulation, iRMB and TripletAttention are close to the original model, only increasing by 0.2%-1.8%. However, the number of parameters of HAttention skyrockets to 21.98×10^6 , which is about 2 times that of the original model. In terms of computation amount (GFLOPs), TripletAttention had the lowest computation amount, only 9.0 GFLOPs, which was significantly reduced by 68.8% compared with the original model. In general, TripletAttention achieves a

balanced performance in terms of accuracy, parameter amount and computational efficiency: the accuracy is the highest (93.7%), the parameter amount is almost unchanged (+0.004%), and the computational amount is reduced the most (-68.8%). Therefore, TripletAttention is finally selected as the attention improvement module of the model.

3.4.3. Improvement and Comparison Experiments of Loss Functions

According to the above experimental results, after improving the model in terms of C2f and attention mechanism, the efficiency of the model has been effectively improved. In order to verify that the loss function is effective for mAP growth, this summary carries out comparative tests of loss functions based on the modified C2f model and the attention mechanism model. And under Focaleriou with the best effect, different parameters are compared. The results are shown in Table 4 below, where the mAP increases by 2.3% and 2% when Inner_CIoU and Inner_Focaleriou are introduced alone. When shape is introduced alone, mAP decreases by 3.1%. In the parameter comparison experiment, when u is 0.85 and ratio is 0.85, the mAP is the highest, reaching 94.2%.

Table 4. Loss function improvement comparison test

Loss function comparison experiment		Parameter comparison experiment		
loss functions	mAP / %	u	ratio	mAP / %
Focaleriou	93.3	0.95	0.7	0.931
shape	87.5	0.9	0.65	93
Inner	93.3	0.85	0.85	94.2
Inner_CIoU	92.9	0.85	0.5	93.1
Inner_Focaleriou	92.6	0.75	0.8	93.4

3.4.4. Ablation Experiment

In order to evaluate the degree of influence of the improved module and its different combination order as well as other algorithms on the experimental accuracy, this section uses the photovoltaic panel defect data set to conduct ablation experiments for verification, and the environment and parameter Settings of the experiments are kept unified. The results of ablation experiments are shown in Table 5 below.

Table 5. Comparison table of ablation experiments

Yolov8	Backbone	C2f	Attention	Loss	Param/($\times 10^6$)	GFLOPs	mAP/%
√	×	×	×	×	11.137535	28.8	90.6
√	√	×	×	×	22.219750	27.4	92.5
√	×	√	×	×	11.302777	8.6	92.3
√	×	×	√	×	11.138435	29.1	93.7
√	×	×	×	√	11.137535	28.8	93.3
√	×	√	√	×	11.701117	8.8	93.4
√	×	√	×	√	11.302777	8.6	93.1
√	×	×	√	√	11.138435	29.1	92.5
√	×	√	√	√	11.701117	8.8	94.2

3.4.5. Comparison Tests of Different Algorithms

In order to verify the effectiveness of the algorithm proposed in this paper, the algorithm is compared with other mainstream algorithms in deep learning. The results are shown in Table 6 below. The proposed method achieves superior detection accuracy while maintaining low computational complexity, demonstrating significant advantages over existing approaches.

Table 6. Comparison of different algorithms in the experimental table

Module	Param/($\times 10^6$)	GFLOPs	mAP/%
Yolov5	9.124127	24.1	91.9
Yolov6	16.306815	44.2	92.9
Yolov8	11.137535	28.8	90.6
Yolov8_SCConv	10.636576	27.7	92.5
Yolov8_RCSOSA	32.133375	90.9	92.7
Yolov8_HGNetV2	30.652831	80.4	92.4
Yolov8_AFPN	6.715417	34.0	90.6
Yolov10	8.070222	24.8	91.9
Rt-Detr	32.816351	108.0	92.4
Yolov11	2.590815	6.4	92.8
Yolov12	9.098399	19.6	92.4
This article	11.701117	8.8	94.2

4. Summary

Aiming at the problem of existing photovoltaic panel defect detection, this paper proposes an improved photovoltaic panel algorithm based on YOLOv8. Based on the Yolov8 model, a series of improvements are carried out, C2f_ODConv is designed in the neck small target layer to improve the feature fusion accuracy, and the TripletAttention attention mechanism is added to strengthen the feature extraction ability of small targets. At the same time, the Focaler-IoU loss is constructed by innovatively combining the Focaler loss function and IoU, which significantly improves the fitting performance of bounding box regression. Experiments show that the proposed algorithm effectively improves the detection accuracy and speed while maintaining the lightweight characteristics of the model, especially strengthens the robustness of the identification of small defects, and provides a more efficient solution for the automatic defect detection of photovoltaic panels.

Experimental results on public datasets show that compared with the original YOLOv8 model, the Computational complexity (GFLOPs) of the proposed algorithm is reduced by 0.7%, and the Average Detection Accuracy (mAP) is increased by 3.8% to 94.2%. Among them, the detection performance of "cover" defects is improved most significantly, and the mAP is increased by 9.1%. The model not only has better overall performance than other mainstream detection networks, but also has the advantages of lightweight and easy deployment. In the actual operation and maintenance of photovoltaic power stations, the algorithm can efficiently detect panel defects, so as to help power stations find problems in time, optimize power generation efficiency, improve system reliability and equipment life. The implementation of automated detection systems offers critical advantages in photovoltaic maintenance operations. This

approach effectively mitigates the inherent hazards associated with manual aerial inspections, thereby substantially reducing workplace safety risks, and has important engineering application value.

Conflicts of Interest

The authors declare that they have no conflict of interest.

References

- [1] YAN Fengyuan. Development of Practical Monitoring Circuit For Photovoltaic Modules[D]. Beijing: North China Electric Power University, 2021.
- [2] Gielen D, Boshell F, Saygin D, et al. The Role of Renewable Energy in the Global Energy Transformation[J]. *Energy Strategy Reviews*, 2019, 24: 38-50.
- [3] LI Bing, ZHAO Kuan, BAI Yunshan, et al. Multi-scale photovoltaic panel defect detection method incorporating attention mechanism[J]. *Electric Power Science and Engineering*, 2023, 39(8): pp. 1-10.(in chinses)
- [4] Y. Guan, G. Wu, W. Huang, J. et al. Gray Level Co-occurrence Matrix-based Defect Detection Method for Photovoltaic Power Plant Panels[C]. 2023 International Conference on Computers, Information Processing and Advanced Education (CIPAE), 2023, 703-707.
- [5] LIAO Kun. Image Recognition and Analysis of Dust Accumulation on Photovoltaic Panels Based on Deep Learning [D]. Northeast Electric Power University, 2020. DOI:10.27008/d.cnki.gdbdc.2020.000092..
- [6] LIU Xiaoxiong, ZHENG Qianying. Research on defect classification and localization algorithm for photovoltaic panels based on deep learning [J]. *Optoelectronic Technology*, 2024, 44(1): pp. 54-60.
- [7] ZHU Chengjie, LIU Lele, ZHU Hongbo.** Multi-scale YOLOv8-MNS Photovoltaic Panel Defect Detection Algorithm [J/OL]. *Journal of Chongqing Technology and Business University (Natural Science Edition)*, 1-9 [2024-11-29]. <http://kns.cnki.net/kcms/detail/50.1155.N.20240604.1406.002.html>.
- [8] WANG Tao, LI Yuansong, SHI Rui, et al. Photovoltaic cell defect detection algorithm based on improved YOLOv8n [J/OL]. *Journal of Chongqing Technology and Business University (Natural Science Edition)*, 1-12 [2025-07-25]. <http://kns.cnki.net/kcms/detail/50.1155.N.20240626.0951.002.html>.
- [9] ZHANG Zijun.** Research on Defect Detection Method of Solar Cell Silicon Modules Based on Faster RCNN [D]. Xiangtan University, 2024. DOI:10.27426/d.cnki.gxtdu.2024.002519.
- [10] YANG Changchun, HE Xuanxuan, WANG Rui, et al.** Photovoltaic Panel Defect Detection Algorithm Based on Improved YOLOv8 [J/OL]. *Electronic Measurement Technology*, 1-13 [2024-11-29]. <http://kns.cnki.net/kcms/detail/11.2175.TN.20241121.1746.066.html>.
- [11] Zhang Z, Liu S, Xiong J. MLCA-YOLO: improved yolov8 for solar cell defect detection[C]. 2024 6th International Conference on Internet of Things, Automation and Artificial Intelligence (IoTAAI), 2024, 24-27.
- [12] GAO Hang, QI Yunsong. Improved YOLOv8n-based defect detection in solar panels [J/OL]. *Infrared Technology*, 1-7 [2025-07-25]. <http://kns.cnki.net/kcms/detail/53.1053.TN.20240923.0931.002.html>.
- [13] HUSSAIN M. YOLO-v1 to YOLO-v8, the rise of yolo and its complementary nature toward digital manufacturing and industrial defect detection[J]. *Ma-chines*, 2023, 11(7): 677.
- [14] TANG Yu, MA Xinna, ZHENG Xuepeng, et al. Multi-source domain rolling bearing fault diagnosis based on ODConv [C]. In: *Nonlinear Vibration Committee, Chinese Society of Vibration Engineering (Ed.), Abstracts of the 19th National Conference on Nonlinear Vibration & 16th National Conference on Nonlinear Dynamics and Motion Stability*. Shijiazhuang: School of Information Science and Technology, Shijiazhuang Tiedao University; State Key Laboratory of Mechanical Behavior and Sys

tem Safety of Traffic Engineering Structures, Shijiazhuang Tiedao University; 2023: p. 300. doi:10.26914/c.cnkihy.2023.112705.

- [15] WENG Junhui, CHENG Le, HUANG Manli, et al. Small target detection in UAV aerial images based on CS-YOLOv5s[J]. *Electronic Measurement Technology*, 2024, 47(7): pp. 157-162. doi:10.19651/j.cnki.emt.2315250.
- [16] Vergura Silvano, Marino Francescomaria. Quantitative and computer-aided thermography-based diagnostics for PV devices: part I—framework[J]. *IEEE Journal of Photovoltaics*, 2017, 7(3): 822-827.